ELSEVIER

Soil Dynamics and Earthquake Engineering 20 (2000) 155–165

SOIL DYNAMICS AND EARTHQUAKE ENGINEERING

www.elsevier.com/locate/soildyn

Evidence of nonlinear site response in HVSR from SMART1 (Taiwan) data

P. Dimitriu[a,*], N. Theodulidis[a], P.-Y. Bard[b]

[a]*Institute of Engineering Seismology and Earthquake Engineering (ITSAK), P.O. Box 53 Finikas, GR-55102 Thessaloniki, Greece*
[b]*Laboratoire de Geophysique Interne et Tectonophysique, P.O. Box 53, F-38041 Grenoble Cedex, France*

Abstract

Deamplification of strong motion and the increase of the effective period of soil deposits are typical nonlinear effects; we seek them in SMART1-array data by applying the horizontal-to-vertical spectral ratio (HVSR) technique. The recordings, from four soil and one rock stations, represent 23 earthquakes (M_L 4.9–7.0); PGA varies between 20–260 cm/s^2. For each station, mean HVSR curves are calculated for two PGA ranges: $<$75 cm/s^2 and $>$100 cm/s^2 (weak and strong motion). At the soil stations, the "weak" (linear) and "strong" (nonlinear) responses are significantly different. Below 1–1.8 Hz, the nonlinear response exceeds the linear one. Above 2 Hz, the nonlinear response drops below the linear one and above 4–6 Hz below unity (deamplification). From 10 to 16 Hz, the two responses converge. One soil site shows significant negative correlation between resonance frequency and ground acceleration. Such behaviour agrees with other empirical studies and theoretical predictions. Our results imply that the HVSR technique is sensitive to ground-motion intensity and can be used to detect and study nonlinear site response.

Keywords: Strong motion; Horizontal-to-vertical spectral ratio; Standard spectral ratio; Nonlinear soil response; Deamplification; Effective resonance frequency

1. Introduction

Seismologists have recently come to recognise something that geotechnical engineers have known for decades, namely the importance of nonlinear effects in site response (e.g. see the review article by Field et al. [1]). This recognition came as a result of a number of "nonlinear" studies, in turn made possible by the availability of a large amount of quality strong-motion data. Nonlinear effects are typically sought by examining the amplitude-dependence of the Fourier spectral ratios between soil and rock surface motions — a technique known as the standard spectral ratio (SSR) method, introduced by Borcherdt [2]. The most characteristic and often cited nonlinear effects are: (1) deamplification of strong motion; and (2) the increase of the effective (resonance) period of soil deposits as the level of excitation increases (e.g. Jarpe et al. [3], Darragh and Shakal [4], Beresnev et al. [5]). Both effects can be expected from theoretical considerations (e.g. Beresnev and Wen [6]) and have been modelled numerically (e.g. Yu et al. [7]).

The application of the SSR method in practice encounters certain important obstacles. First, a suitable reference (rock) site is often difficult to find in the vicinity of the soil site of interest (e.g. Cranswick [8], Steidl et al. [9], Boore and Joyner [10]). And second, the spatial separation of the soil and rock sites requires correcting the recordings for path and finite-source effects (e.g. Field et al. [11]). Therefore, another nonreference-site technique — the horizontal-to-vertical spectral ratio (HVSR) method — has been lately gaining popularity in site-response analyses (e.g. Theodulidis and Bard [12]; Theodulidis et al. [13], Chavez-Garcia et al. [14], Lachet et al. [15], Bonilla et al. [16], Raptakis et al. [17], Dimitriu et al. [18]). Yet the question remains open whether this technique is sensitive to the amplitude of the ground motion and hence can be used to assess nonlinear site response. In a recent study, Dimitriu et al. [19] applied the HVSR method to (mostly near-field) acceleration data recorded at a soil site in the town of Lefkas (on Lefkas Island, Ionian Sea, western Greece) and found an impressive increase in the site's effective resonance period with increasing excitation level. No accompanying deamplification of strong motion relative to weak motion was noticed. These results were attributed to the nonlinear behaviour (shear-modulus degradation) of the surface soft sandy-silt layer.

In the present study we apply the HVSR technique to data from five stations (four soil and one rock) of the SMART1

* Corresponding author. Tel.: +30-31-476081; fax: +30-31-476085.
E-mail address: pedim@itsak.gr (P. Dimitriu).

0267-7261/00/$ - see front matter
PII: S0267-7261(00)00047-6

Table 1
1D soil profile near station O07 used in linear modelling of Fig. 4. Adapted from Wen [20]; Q-values and densities are assumed

Depth (m)	V_S (m/s)	Q_S	V_P (m/s)	Q_P	Density (kg/m^3)
(a) *Linear*					
0	120	20	370	50	1800
5	140	25	810	100	1800
8	190	30	1270	130	1800
13	220	35	1330	150	1800
34	250	40	1250	130	1800
48	270	40	1220	130	1800
60	320	50	1470	150	1800
80	480	70	1540	200	1800
150	600	100	1900	250	2000
250	1500	150	3700	400	2500
(b) Nonlinear					
0	75	10	370	50	1800
12	110	25	810	100	1800
18	180	30	1270	130	1800
48	270	40	1330	150	1800
60	320	50	1470	150	1800
80	480	70	1540	200	1800
150	600	100	1900	250	2000
250	1500	150	3700	400	2500

accelerograph array in Taiwan. The data cover a wide range of earthquake magnitudes, epicentral distances and peak ground accelerations (PGA). Our purpose is to try to detect nonlinear effects of the "deamplification" and "effective-frequency-reduction" kinds while testing the findings of the Dimitriu et al. [19] study in a different geologic and seismotectonic environment.

2. Geologic, strong-motion and earthquake data

The SMART1 accelerograph array is located on the Lanyang plain in northeast Taiwan and begun operation in September 1980. The array, the strong-motion data it collected and the corresponding earthquake catalogue are reviewed in Abrahamson et al. [20]. Local geology and site conditions in the area are presented by Wen [21] and Yeh and Wen [22] (Table 1). Numerous studies have made use of SMART1 data, focusing on specific aspects of the site-response problem, including the spatial variability of strong ground motion (Beresnev et al. [23]) and nonlinear soil behaviour (e.g. Wen [21], Beresnev et al. [24]).

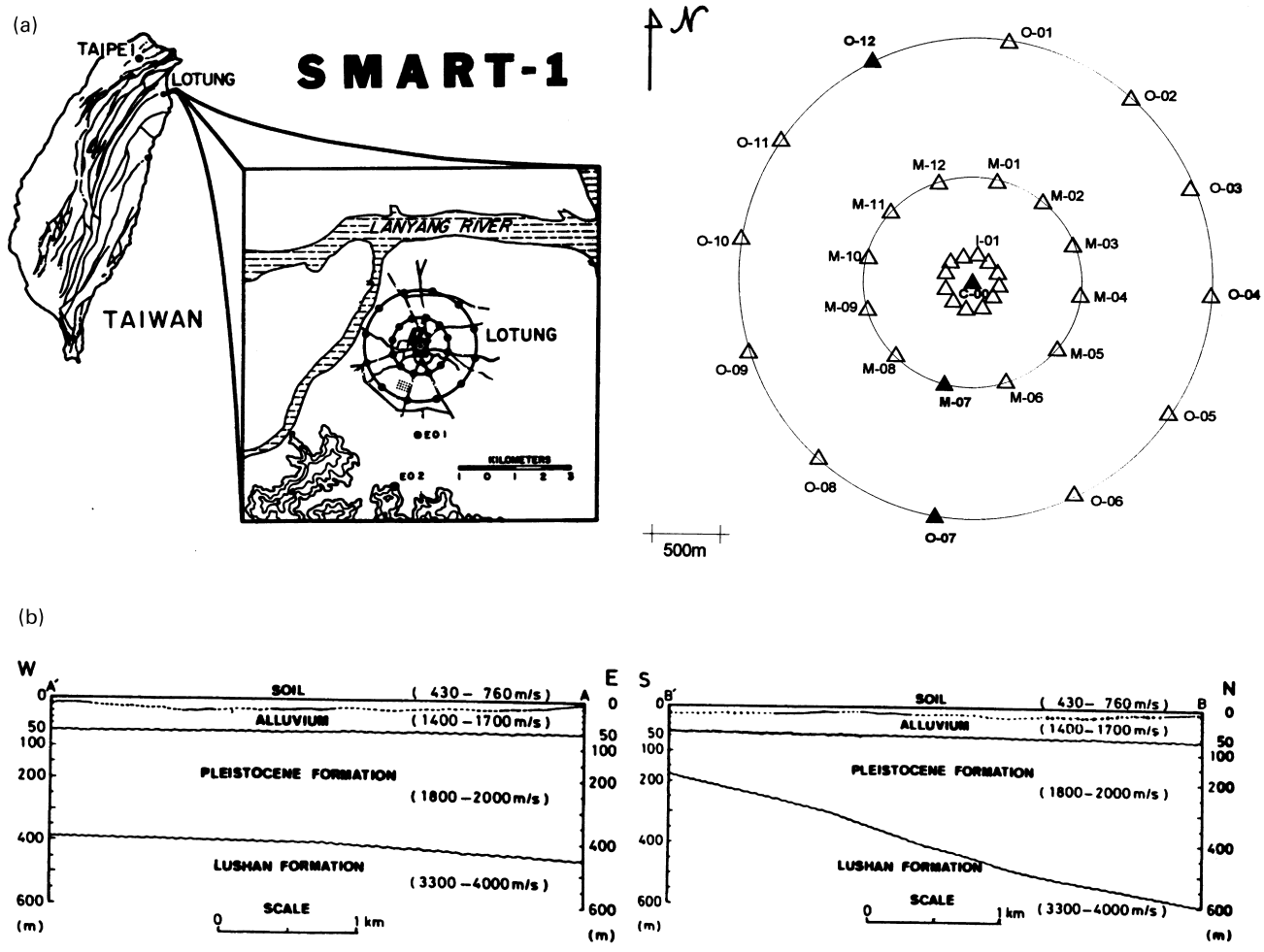

Fig. 1. SMART1 array (a) and schematic geology of the Lanyang plain (b). Black triangles represent the four soil stations studied. The fifth station, E02 is on robust-rock outcropping. (Adapted from Theodulidis et al. [12]).

Table 2
Information on the earthquakes whose recordings used. R is epicentral distance from the array's central station, C00 (see Fig. 1). Last column lists stations whose recordings are used. (Adapted from Abrahamson et al. [19])

No	Date Da/Mo/Ye	Lat. N	Long. E	Depth (km)	M_L	R (km)	Stations				
02	14/11/80	24.61	121.75	78	6.1	7	O12	C00			
05	29/01/81	24.44	121.92	25	5.7	30	O12	C00	M07	O07	
14	30/08/81	24.50	121.93	20	5.0	26			M07		
18	28/02/82	24.81	121.92	15	5.1	22		C00	M07		
19	01/04/82	24.58	122.10	17	4.9	36			M07		
20	17/12/82	24.56	122.53	88	6.4	88	O12		M07	O07	
22	10/05/83	24.50	121.52	19	6.4	31	O12	C00	M07	O07	
23	21/06/83	24.13	122.39	43	6.6	87			M07		
24	24/06/83	24.17	122.39	48	6.9	84	O12	C00	M07	O07	
25	21/09/83	24.08	122.16	44	6.8	68	O12				E02
28	18/04/84	24.91	122.54	16	5.9	83				O07	
29	23/04/84	24.94	122.11	28	6.0	46	O12		M07	O07	
30	29/12/84	24.78	122.02	88	6.3	28	O12	C00	M07	O07	
31	09/03/85	24.76	122.23	4	5.9	48		C00			
33	12/06/85	24.57	122.19	3	6.5	45		C00	M07	O07	E02
35	12/08/85	24.71	121.79	8	5.7	5		C00			E02
39	16/01/86	24.76	121.96	10	6.5	22	O12	C00	M07	O07	E02
40	20/05/86	24.08	121.59	16	6.5	67	O12	C00	M07	O07	E02
41	20/05/86	24.05	121.62	22	6.2	71	O12	C00	M07	E02	O07
42	17/07/86	24.66	121.82	2	5.0	5	O12	C00	M07	O07	E02
43	30/07/86	24.63	121.79	2	6.2	6	O12	C00	M07	O07	E02
44	30/07/86	24.64	121.80	2	4.9	5	O12	C00	M07	O07	
45	14/11/86	23.96	121.84	7	7.0	79	O12	C00	M07	O07	E02

Table 3
Horizontal peak ground accelerations (PGA, absolute value in cm/s^2) of the recordings used (see Table 1). N and E stand for the NS and EW components, respectively. To ensure an acceptable signal/noise ratio, recordings with PGA $>$ 20 cm/s^2 were typically used. In bold type are the 'strong-motion' recordings (PGA $>$ 100 cm/s^2); the rest are 'weak-motion' ones (PGA $<$ 75 cm/s^2). Three recordings with intermediate PGA were discarded (italic type)

Event	Station									
	O12		C00		M07		O07		E02	
	PGA-N	PGA-E	PGA-N	PGA-E	PGA-N	PGA-E	PGA-N	PGA-E	PGA-N	PGA-E
02	33	52	50	57						
05	**162**	**87**	**112**	**97**	**107**	**111**	*80*	*85*		
14			30	17	35	21				
18			61	47	26	28				
19					20	21				
20	44	37			44	56	43	45		
22	34	37	51	31	58	48	41	39		
23					24	23				
24	41	32	58	40	41	36	46	34		
25	23	22							19	19
28							28	60		
29	24	36			27	46	50	73		
30	24	32	34	30			36	26		
31			28	43						
33			34	37	29	53	47	62	30	21
35			52	62					29	20
39	**125**	**95**	**210**	**198**	**258**	**156**	**170**	**157**	**199**	**157**
40	**149**	**87**	**230**	**170**	**250**	**180**	**162**	**158**	**96**	**186**
41	33	17	51	51	40	42	31	19	49	33
42	49	25	*80*	*78*	68	57	64	*108*	68	53
43	**149**	**120**	**152**	**116**	**127**	**197**	**105**	**137**	**246**	**183**
44	29	23	47	32	41	66	36	17		
45	**155**	**137**	**134**	**121**	**118**	**152**	**107**	**100**	**137**	**133**

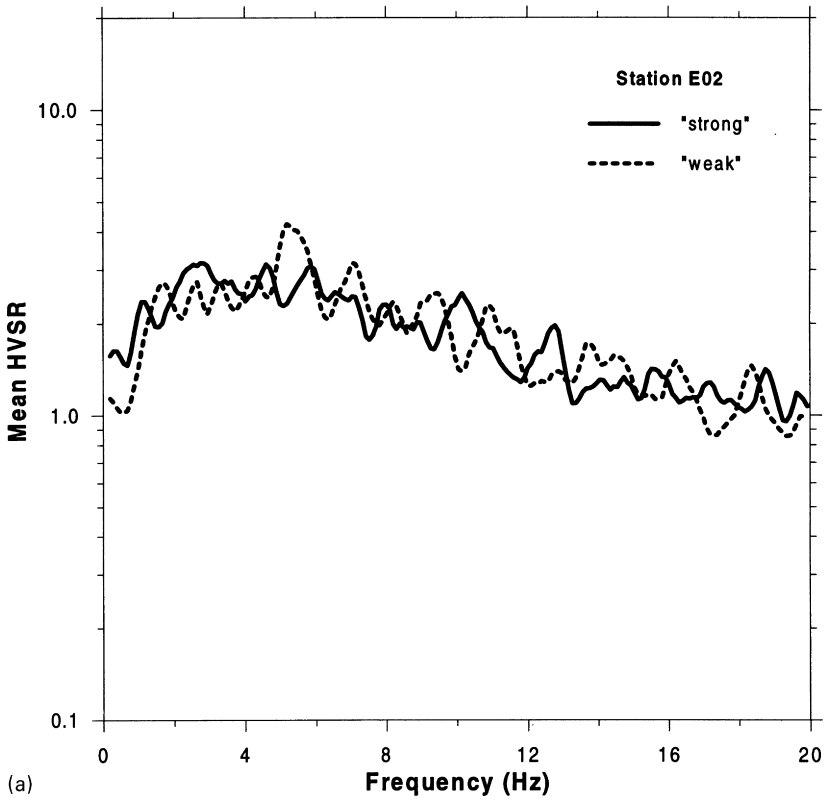

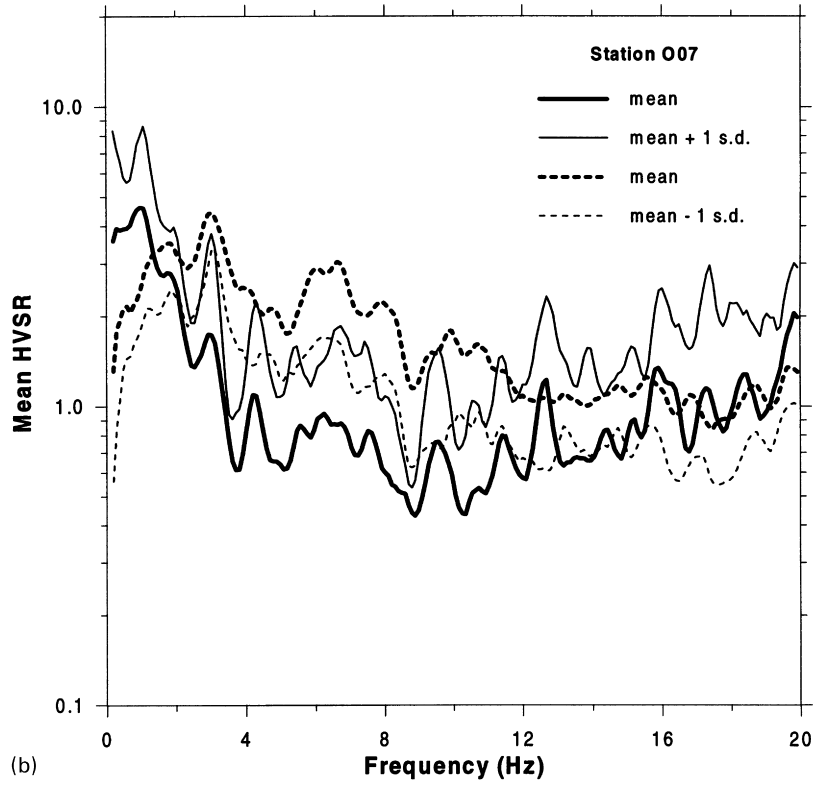

Fig. 2. "Strong" (PGA > 100 cm/s^2; continuous lines) and "weak" (PGA < 75 cm/s^2; interrupted lines) mean HVSR curves at the five sites, from South to North: E02 (rock) (a), O07 (b), M07 (c), C00 (array's central station) (d) and O12 (e) (see Fig. 1).

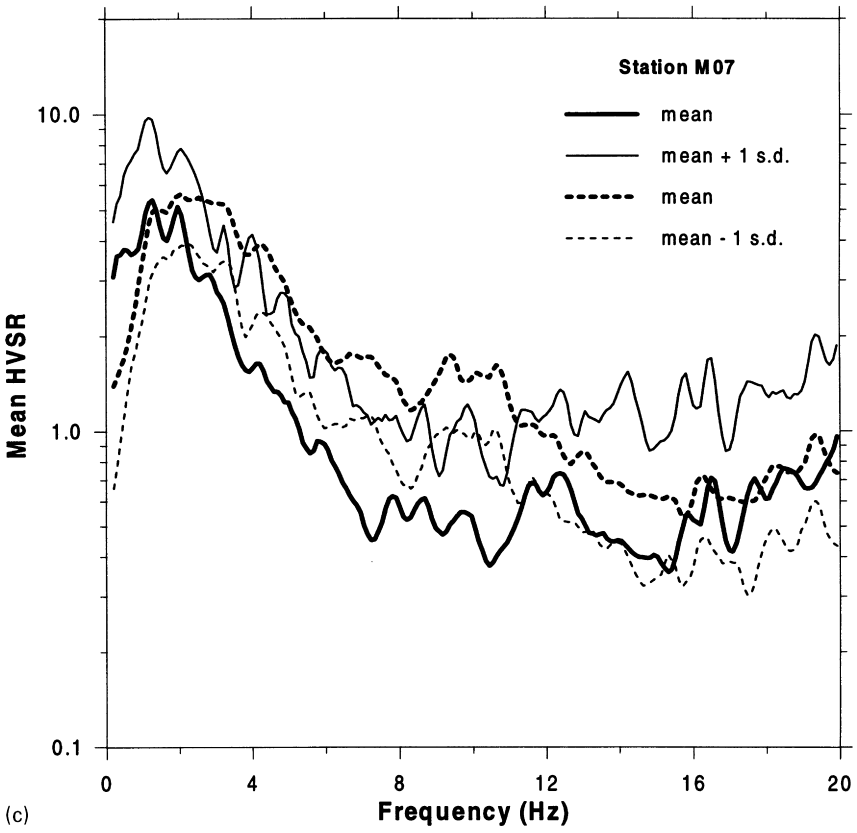

(c)

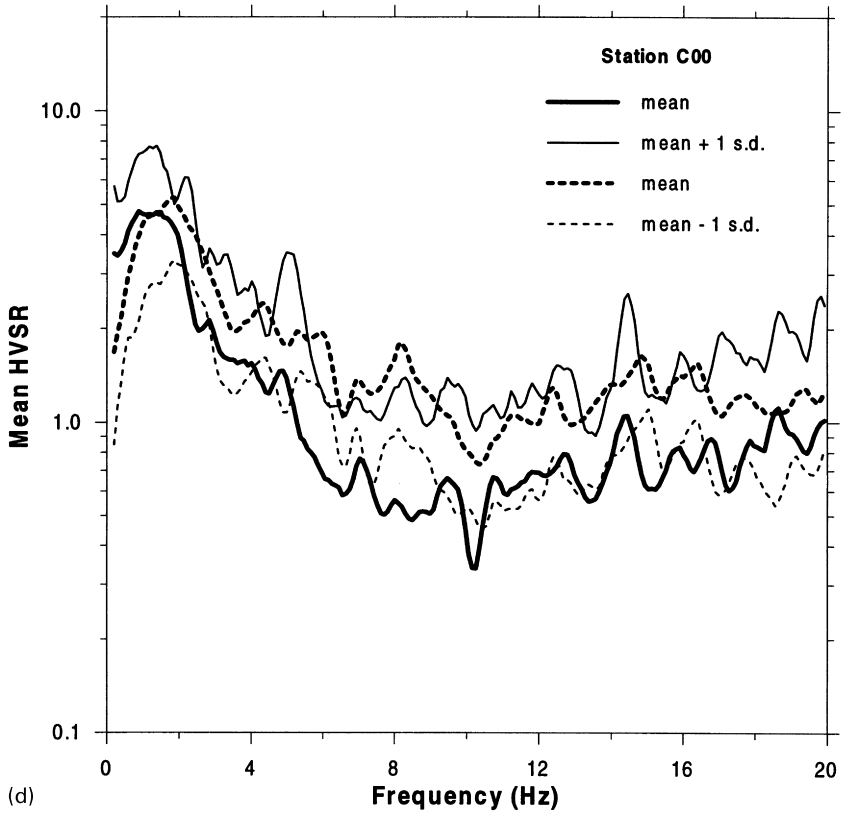

(d)

Fig. 2. (*continued*)

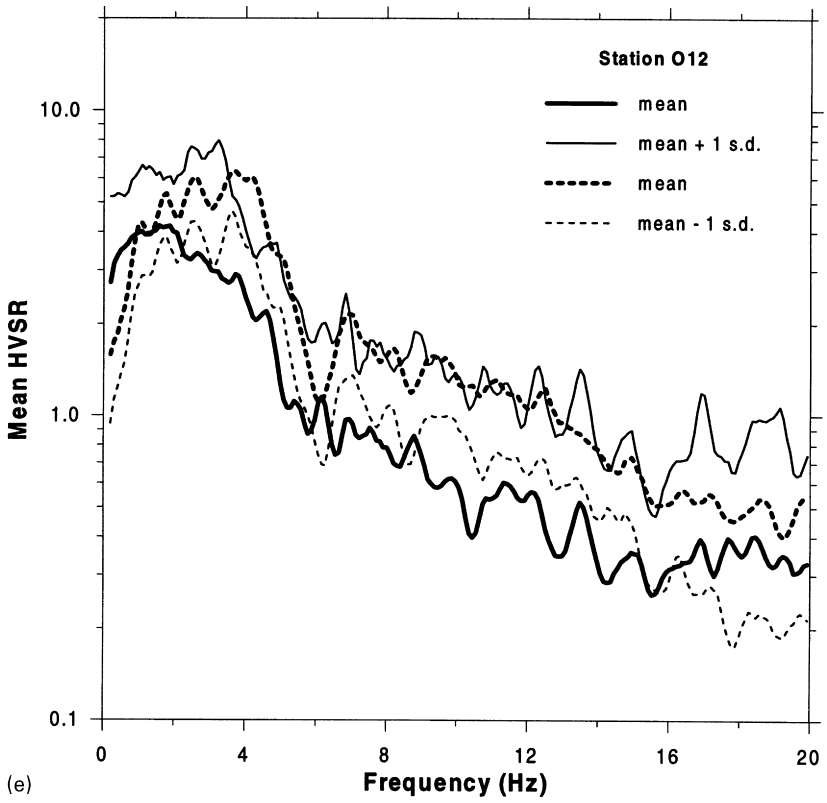

Fig. 2. (*continued*)

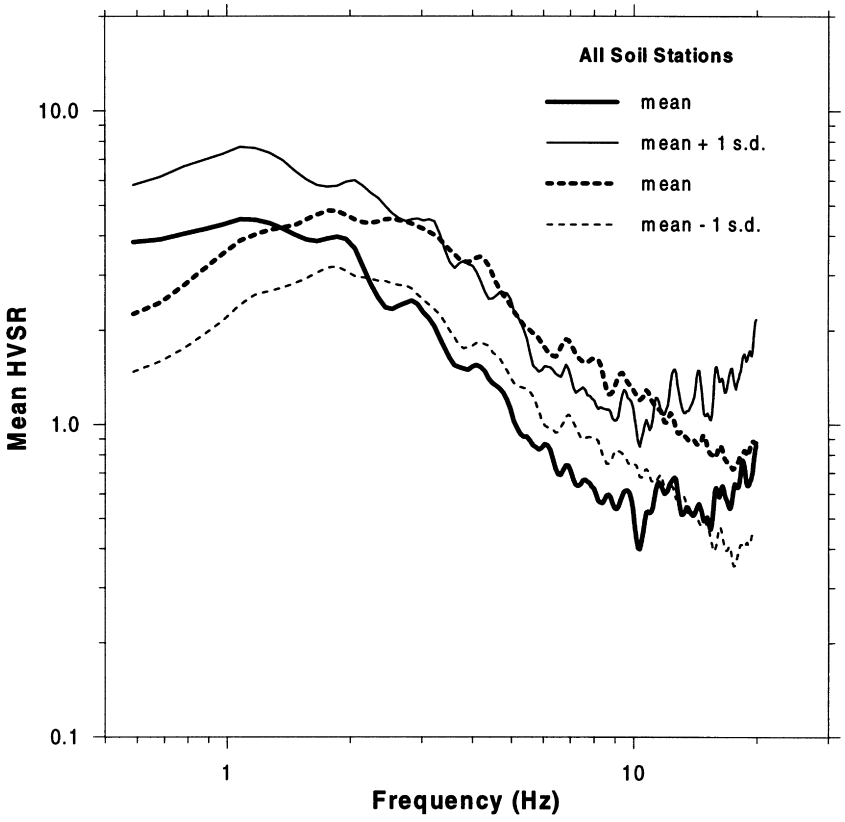

Fig. 3. "Strong" (PGA $>$ 100 cm/s^2) and "weak" (PGA $<$ 75 cm/s^2) mean HVSR curves for the four soil sites, O07, M07, C00 and O12, considered to belong to one category. Log–log plot facilitates comparison with Fig. 5 of Beresnev et al. [24], showing mean SSR curves for all array soil stations and a different weak-motion dataset. Same notations as in Fig. 2.

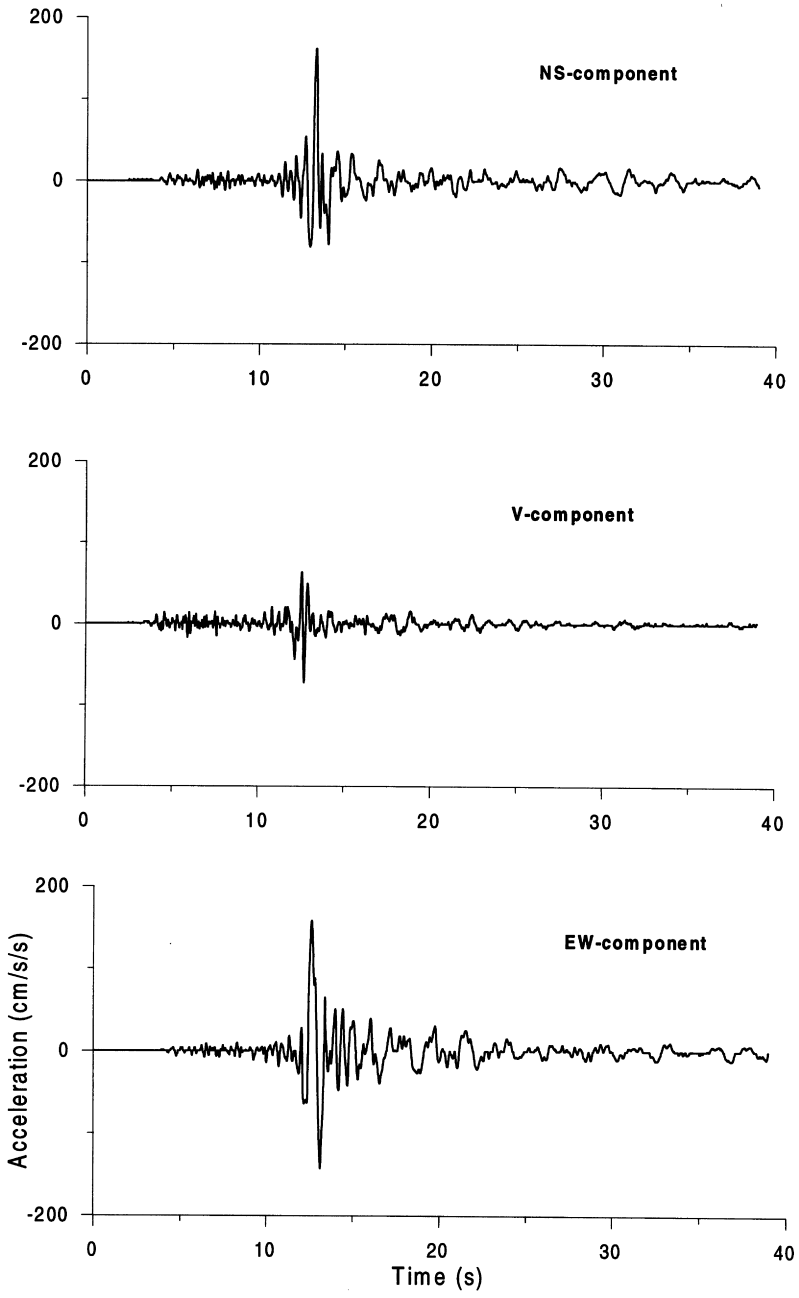

Fig. 4. Accelerogram of event 40 (Table 3), recorded at station O07 and used in correlation analysis between the site's resonance frequency and PGA and "mean" acceleration (Fig. 5).

SMART1 data are 3-component digital accelerograms sampled every 0.01 s; the working frequency range is 0.1–25 Hz (Abrahamson et al. [20]). Here we use recordings from five stations placed along a line crossing the array in the NS direction (Fig. 1a). One station (E02) is located on robust-rock outcrop and the others on soil. The geology of the plain consists of recent alluvium with roughly constant thickness overlying Pleistocene materials with increasing thickness (from S to N) and Miocene rock (Fig. 1b).

The earthquake and strong-motion data are listed in Tables 2 and 3; station codes are the same as given in Abrahamson et al. [20]. The recordings used have peak horizontal accelerations (PGA) in the range 20–260 cm/s^2 (weaker recordings were rejected to ensure an acceptable signal-to-noise ratio) and represent a total of 23 earthquakes with M_L magnitude from 4.9 to 7.0 that occurred between November 1980 and November 1986. The events cover a wide range of epicentral distances and azimuths, respectively, 5–88 km and 46–212° (measured relative to the array's central station, C00).

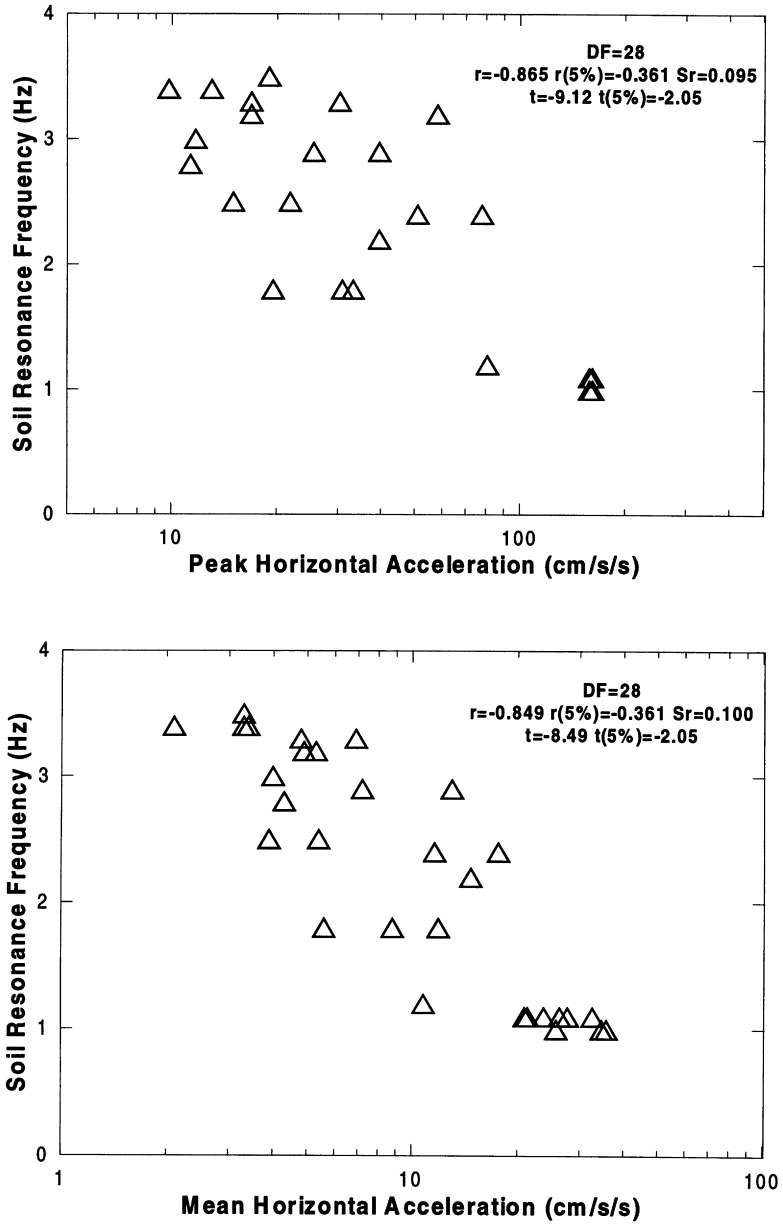

Fig. 5. Results of linear correlation analysis between site-O07 effective resonance frequency (f_{res}), determined visually from HVSR curves for 15 subsequent overlapping 5.12-s windows of event-40 accelerogram, and the corresponding values of: (a) PGA; and (b) "mean" acceleration (the mean of absolute acceleration values). DF is number of degrees of freedom (= 28); r is correlation coefficient (S_r — standard error); t is Student's t-test statistic; r (5%) and t (5%) are values of the statistics at the 5% confidence level.

3. Method

For each recording considered, Fourier amplitude spectra of acceleration were computed from 10.24-s windows starting before and including the strongest (S-wave) arrivals and were smoothed with a 0.4-Hz triangular window (sufficient smoothing preserving the spectral shape). For each station, spectral ratios between the horizontal components and the vertical component of each recording (HVSR) were computed, and then mean HVSR curves were calculated for two PGA ranges: <75 cm/s^2 and >100 cm/s^2 (weak and strong motion, respectively). At station O07, exhibiting a clear shift in resonance frequency, f_{res}, between the two PGA ranges, we checked for a possible correlation between f_{res} and ground acceleration (peak and mean values) by examining HVSR from subsequent 5.12-s windows of a suitable recording (sufficient length and range of acceleration values).

4. Results

The mean HVSR curves for the two PGA ranges, <75 cm/s^2 and >100 cm/s^2 (weak and strong motion) for

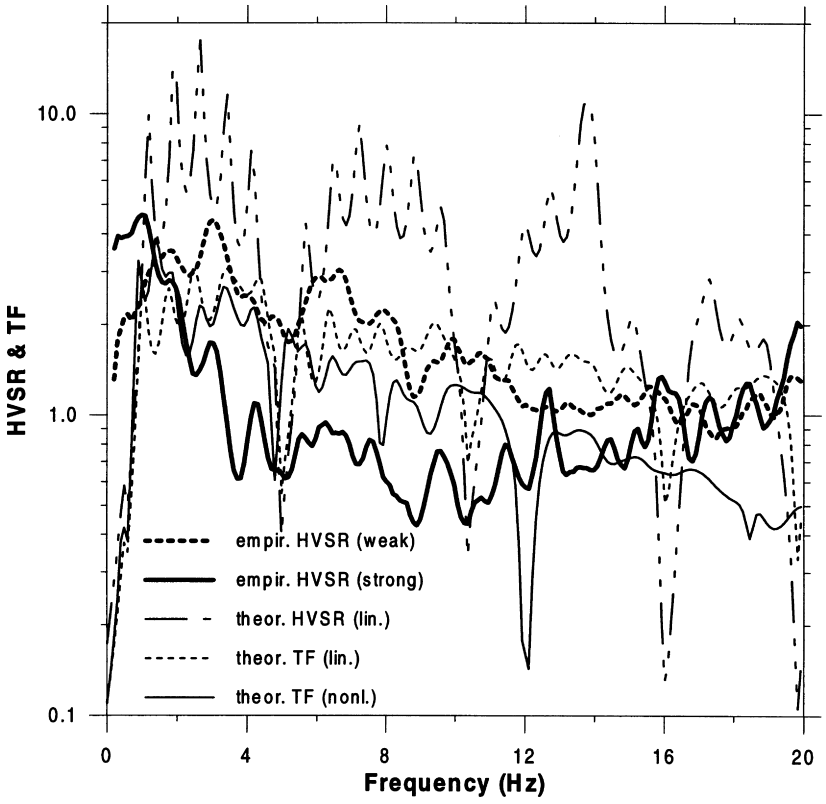

Fig. 6. Comparison of empirical mean HVSR curves ("strong" and "weak") for station O07 with theoretical HVSR and soil- to rock-surface amplification curves (TF) computed by Kennett's technique (Kennett and Kerry [25]) for an SV-wave incidence at 50° (from the vertical) to the soil/rock interface; the ("linear" and "nonlinear") soil structures used are shown in Table 1, adapted from Wen [22].

the stations considered, from the southernmost one, on robust-rock outcrop (E02), to the northernmost one (O12) (see Fig. 1), are displayed in Fig. 2. We remind that the deposit thickness increases from South to North (Fig. 1b). Given the similarity of the results for the individual soil stations, we computed mean "strong" and "weak" curves for the four soil sites, considered to belong to one category (Fig. 3). The log–log format in Fig. 3 was used to facilitate comparison with Fig. 5 of Beresnev et al. [24], showing average soil-to-rock spectral ratios (SSR) for all SMART1-array soil stations. Unlike us, Beresnev et al. [24] applied the SSR technique and used fewer weak-motion recordings per station.

At the O07 site, presenting a clear shift in the (effective) resonance frequency, f_{res}, between the "strong" and "weak" mean responses (Fig. 2b), we determined f_{res} from HVSR curves computed for 15 subsequent (overlapping) 5.12-s windows of the recording of event 40 (Fig. 4; see Table 3). Fig. 5 presents the results of linear correlation analysis between f_{res} and, in turn, PGA and "mean" acceleration (the mean of the absolute acceleration values) in each window. To each window there correspond two pairs of values of the variables (one for each horizontal component of the recording).

Finally, we compare the empirical HVSR curves for station O07 with the theoretical HVSR and soil- to rock-surface transfer function computed by running an implementation of Kennett's (see Kennett and Kerry [25]) 1D linear method for an SV-wave incident at 50° (from the vertical) at the soil/rock boundary for two soil structures: "linear" and "nonlinear" (Table 1) (Fig. 6). The angle of 50° is representative of shallow near-field earthquakes as well as more distant ones (e.g. Seale and Archuleta [26]).

5. Discussion and conclusion

5.1. Deamplification

Strictly speaking, deamplification is the phenomenon where amplification (or transfer) function assumes values under unity. In the nonlinear literature, the term also indicates that the strong motion is amplified less than the weak motion. This effect has been observed in spectral ratios between soil- and rock-surface motions (SSR technique) in many diverse geologic and seismotectonic environments, including the SMART1-array area (Beresnev et al. [24]). Although Beresnev et al. [24] used a different methodology and a different dataset (all array stations but fewer weak-motion recordings per station), their array-averaged soil-to-rock amplification curves are remarkably similar to our (mean) HVSR amplification curves (cf. their Fig. 5 with

our Fig. 3). Thus, in both cases, the effect of the nonlinearity can be divided into three distinct frequency bands. Till about 1.3–1.8 Hz, the strong-motion (nonlinear) response exceeds the weak-motion (linear) one. Above ca. 2 Hz, the nonlinear response falls below the linear one and above ca. 4 Hz drops under unity (deamplification). From about 10 Hz, the two responses converge. Qualitatively identical behaviour is obtained in numerical simulations of the nonlinear response of soil deposits (e.g. Yu et al. [7]). Even linear modelling, with soil parameters modified according to their "nonlinear" values (Table 1), seems to capture the main qualitative features (deamplification and resonance-frequency reduction) of the nonlinear response (Fig. 6). Significantly, there is practically no difference between the strong- and weak-motion responses of the rock site (Fig. 2a).

5.2. Reduction of the effective (resonance) frequency

Reduction of the effective (resonance) frequency of soil deposits with increasing level of excitation can be expected on the basis of theoretical considerations (e.g. Beresnev and Wen [6]). Thus degradation of the soil's shear modulus with increasing strain leads to a decrease of the effective shear-wave velocity and hence to a reduction of the effective (resonance) frequency of the soil deposit. Conclusive evidence that this nonlinear effect occurs was presented by Beresnev et al. [5], again with the aid of the SSR technique.

Using the HVSR technique, Dimitriu et al. [19] also observed a considerable drop of the effective resonance frequency of a soil site with simple geology in the town of Lefkas in western Greece and linked it, both qualitatively and quantitatively, to the nonlinear behaviour (shear-modulus degradation) of the top sandy-silt layer. Furthermore, significant correlation was found between f_{res} and PGA and PGV (r between -0.7 and -0.8). Our correlation analysis for station O07 is in remarkable agreement with the above results (Fig. 5). In contrast, the data from the other soil stations seem to lend support to Yu et al.'s [7] conclusion — based on numerical modelling — that the apparent decrease in the effective frequency is caused primarily by deamplification of shorter-period waves rather than by amplification of long-period motion (see Fig. 2c–e). Whereas there is no contradiction between the two interpretations, as both nonlinear effects — deamplification and effective-frequency reduction — act simultaneously, their relative significance seems to depend on the properties of the soil deposit, particularly the degree of nonlinearity and the existence of a clear dominant resonance. Very importantly, and in accordance with the results of Dimitriu et al. [19], linear 1D modelling accounts, at least in part, for the observed shift in resonance frequency between the "strong" and "weak" HVSR (Fig. 6).

In conclusion, the application of the HVSR method to SMART1 data has provided evidence for the nonlinear effect of deamplification of strong ground motion (PGA > 100 cm/s^2) relative to comparatively weaker motion (PGA < 75 cm/s^2). At one soil site there is also clear indication of a significant shift in the dominant (resonance) frequency, which strongly negatively correlates with the intensity of ground motion (PGA and "mean" acceleration). These results agree with other empirical studies, conform to nonlinear theory and enforce the suggestion of Dimitriu et al. [19] that the HVSR technique is capable of detecting nonlinear effects and can be used to assess site response during strong shaking. In particular, our results imply that, depending on the frequency band, nonlinear soil behaviour has a different influence on HVSR, ranging from relative amplification at low frequencies to deamplification at higher frequencies. Moreover, for sites exhibiting a clear resonance, the resonance frequency decreases with increasing excitation level.

References

[1] Field EH, Kramer S, Elgamal A-W, Bray JD, Matasovic N, Johnson PA, Cramer C, Roblee C, Wald DJ, Bonilla LF, Dimitriu PP, Anderson JG. Nonlinear site response: where we're at. Seismol Res Lett 1998;69:230–4.
[2] Borcherdt RD. Effects of local geology on ground motion near San Francisco Bay. Bull Seismol Soc Am 1970;60:29–61.
[3] Jarpe SP, Cramer CH, Tucker BE, Shakal AF. A comparison of observations of ground response to weak and strong ground motion at Coalinga, California. Bull Seismol Soc Am 1988;78:421–35.
[4] Darragh RB, Shakal AF. The site response of two rock and soil station pairs to strong and weak ground motion. Bull Seismol Soc Am 1991;81:1885–99.
[5] Beresnev IA, Field EH, Van Den Abeele K, Johnson PA. Magnitude of nonlinear sediment response in Los Angeles basin during the 1994 Northridge, California, earthquake. Bull Seismol Soc Am 1998;88:1079–84.
[6] Beresnev IA, Wen K-L. Nonlinear soil response — a reality?. Bull Seismol Soc Am 1996;86:1964–78.
[7] Yu G, Anderson JG, Siddharthan R. On the characteristics of nonlinear soil response. Bull Seismol Soc Am 1992;83:218–44.
[8] Cranswick E. The information content of high-frequency seismograms and the near-surface geologic structure of hard rock recording sites. Pageoph 1988;128:335–63.
[9] Steidl JH, Tumarkin AG, Archuleta RJ. What is a reference site?. Bull Seismol Soc Am 1996;86:1733–48.
[10] Boore DM, Joyner BW. Site amplification for generic rock sites. Bull Seismol Soc Am 1997;87:327–41.
[11] Field EH, Johnson PA, Beresnev IA, Zeng Y. Nonlinear ground-motion amplification by sediments during the 1994 Northridge earthquake. Nature 1997;390:599–602.
[12] Theodulidis N, Bard P-Y. Horizontal to vertical ratio and geological conditions: an analysis of strong motion data from Greece and Taiwan (SMART-1). Soil Dyn Earthquake Engng 1995;14:177–97.
[13] Theodulidis N, Archuleta RJ, Bard P-Y, Bouchon M. Horizontal-to-vertical spectral ratio and geological conditions: the case of Garner Valley downhole array in southern California. Bull Seismol Soc Am 1996;86:306–19.
[14] Chavez-Garcia FJ, Sanchez LR, Hatzfeld D. Topographic site effects and HVSR: a comparison between observations and theory. Bull Seismol Soc Am 1996;86:1559–73.
[15] Lachet C, Hatzfeld D, Bard P-Y, Theodulidis N, Papaioannou Ch, Savvaidis A. Site effects and microzonation in the city of Thessaloniki (Greece): comparison of different approaches. Bull Seismol Soc Am 1996;86:1692–703.
[16] Bonilla FL, Steidl JH, Lindley GT, Tumarkin AG, Archuleta RJ. Site

amplification in the San Fernando Valley, CA: variability of site effect estimation using the S-wave, coda and H/V methods. Bull Seismol Soc Am 1997;87:710–30.

[17] Raptakis D, Theodulidis N, Pitilakis K. Data analysis of the Euro-seistest strong motion array in Volvi (Greece): standard and horizontal-to-vertical spectral ratio techniques. Earthquake Spectra 1998;14:203–24.

[18] Dimitriu PP, Papaioannou ChA, Theodulidis NP. EURO-SEISTEST strong-motion array near Thessaloniki, Northern Greece: a study of site effects. Bull Seismol Soc Am 1998;88:862–73.

[19] Dimitriu PP, Kalogeras I, Theodulidis N. Evidence of nonlinear site response in horizontal-to-vertical spectral ratio from near-field earthquakes. Soil Dyn Earthquake Engng 1999;18:423–35.

[20] Abrahamson NA, Bolt BA, Darragh RB, Penzien J, Tsai YB. The SMART I accelerograph array (1980–1987): a review. Earthquake Spectra 1987;3:263–87.

[21] Wen K-L, Yeh YT. Seismic velocity structure beneath the SMART-1 array. Bull Inst Earth Sci, Academia Sinica 1984;4:51–72.

[22] Wen K-L. Nonlinear soil response in ground motions. Earthquake Engng Struct Dyn 1994;23:599–608.

[23] Beresnev IA, Wen K-L, Yeh YT. Source, path and site effects on dominant frequency and spatial variation of strong ground motion recorded by Smart1 and Smart2 arrays in Taiwan. Earthquake Engng Struct Dyn 1994;23:583–98.

[24] Beresnev IA, Wen K-L, Yeh YT. Nonlinear soil amplification: its corroboration in Taiwan. Bull Seismol Soc Am 1995;85:496–515.

[25] Kennett BL, Kerry NJ. Seismic waves in stratified halfspace. Geophys J R Astr Soc 1979;57:557–83.

[26] Seale SH, Archuleta RJ. Site amplification and attenuation of strong ground motion. Bull Seismol Soc Am 1989;79:1673–96.